



Crosslinked superhydrophobic films fabricated by simply casting poly(methyl methacrylate-butyl acrylate-hydroxyethyl methacrylate)-b-poly(perfluorohexylethyl methacrylate) solution

Xiufang Wen^a, Chao Ye^a, Zhiqi Cai^b, Shouping Xu^a, Pihui Pi^{a,*}, Jiang Cheng^a, Lijuan Zhang^a, Yu Qian^a

^a The School of Chemistry and Chemical Engineering, South China University of Technology, Guangzhou 510640, PR China

^b Shaoguan Institute, Jinan University, Shaoguan City 512026, PR China



ARTICLE INFO

Article history:

Received 9 January 2015

Received in revised form 10 February 2015

Accepted 11 February 2015

Available online 3 March 2015

Keywords:

Crosslinked superhydrophobic films

Block polymer

Micelle solution

Mixed solvent

ABSTRACT

This study focuses on the preparation of superhydrophobic films by crosslinkable polymer material-Poly(methyl methacrylate-butyl acrylate-hydroxyethyl methacrylate)-b-Poly(perfluorohexylethyl methacrylate) (P (MMA-BA-HEMA)-b-PFMA) with a simple one-step casting process. Nanoscale micelle particles with core-shell structure was obtained by dissolving the polymer and curing agent in the mixture of acetone and 1H, 1H, 5H octafluoropentyl-1,1,2,2 tetrafluoroethyl ether (FHT). Superhydrophobic films were fabricated by casting the micelle solution on the glass slides. By controlling the polymer concentration and acetone/FHT volume ratio, superhydrophobic polymer film with water contact angle of $153.2 \pm 2.1^\circ$ and sliding angle of 4° was obtained. By introducing a curing agent into the micelle solution, mechanical properties of the films can be improved. The adhesion grade and hardness of the crosslinked superhydrophobic films reached 2 grade and 3H, respectively. The hydrophobicity is attributed to the synergistic effect of micro–submicro–nano-meter scale roughness by nanoscale micelle particles and low surface energy of fluoropolymer. This procedure makes it possible for widespread applications of superhydrophobic film due to its simplicity and practicability.

© 2015 Elsevier B.V. All rights reserved.

1. Introduction

Superhydrophobic surfaces, defined as surfaces with a water contact angle (WCA) larger than 150° and low contact angle hysteresis, have attracted considerable attentions in recent years [1]. This type of surface has been widely used in applications including antifogging, self-cleaning, anticorrosion, water harvesting, etc. [2–4]. It has been revealed that a peculiar topology based on micro- and nanoscopic surface roughness combined with the hydrophobic properties of its epicuticular wax is a prerequisite for superhydrophobic film [5]. Considerable efforts have been focused on the development of superhydrophobic surfaces through the design of proper roughness. Various approaches, based on sol–gel [5–8], the sublimation of aluminum acetylacetone [9], lithography [10], spinning [11], chemical etching [12] and others [13–15] were reported.

Among these methods, polymer film casting, such as fluorinated copolymer [16] and polystyrene [11], have been proved to be a scalable methodology. For example, block copolymer were used to prepared superhydrophobic films through phase separation to form surface with variable morphology [17]. Xie et al. prepared a superhydrophobic surface by casting a micelle solution of the diblock copolymer of polypropylene-b-poly(methyl methacrylate), under an ambient atmosphere [18,19]. Deepak and Asha revealed that a polymer possessing both bulky units and polar structures as side chains could self-organize when a certain amount of water was added to the polymer solution for phase separation [20]. In our previous study, a block copolymer-poly(methyl methacrylate-butyl methacrylate-hydroxyethyl methacrylate)-b-Poly(perfluorohexylethyl methacrylate) (P (MMA-BMA-HEMA)-b-PFMA) was used to fabricate hydrophobic surfaces [21]. However, major challenge remains in developing scalable methodologies that enable superhydrophobic coatings on versatile substrates with a combination of strong mechanical and chemical stability, etc. [22].

In this paper, we prepared a crosslinked superhydrophobic surface with good mechanical performance. A fluorinated block copolymer, poly(methyl methacrylate-butyl

* Corresponding authors. Fax: +86 20 87112057 804.
E-mail address: phpi@scut.edu.cn (P. Pi).

acrylate-hydroxyethyl methacrylate)-b-poly(perfluorohexylethyl methacrylate) (P(MMA-BA-HEMA)-b-PFMA) was synthesized using a typical ATRP method. By mixing this copolymer in acetone and 1H, 1H, 5H octafluoropentyl-1,1,2,2-tetrafluoroethyl ether (FHT), micelles with core-shell structure was obtained. The micelle was cast onto clean glass to prepare superhydrophobic film by self-assembly of the fluorinated block copolymer. Curing agent of tolulene diisocyanate (L75) was introduced into micelle solution to improve the adhesion and hardness of film through crosslinking reaction between hydroxyl groups of the fluorinated block copolymer and -NCO groups of L75. The superhydrophobic films improve mechanical performance that satisfies practical application (e.g. self-cleaning) and have good potential application prospects.

2. Experimental

2.1. Synthesis of the fluorinated block copolymer

P(MMA-BA-HEMA)-b-PFMA was obtained from macro-initiator (P(MMA-BA-HEMA)-Br) and FMA according to the procedure outlined in **Scheme 1**. Firstly, a typical ATRP was carried out as follows. A mixture of MMA (2.00 g, 20 mmol), BA (10.14 g, 30 mmol), HEMA (1.3 g, 10 mmol), ligand (PMDETA) and solvent (xylene, dimethyl-formamide (DMF) or cyclohexanone) was added to a 50 mL Schlenk flask equipped with a rubber septum and a stirring bar, and degassed by three freeze–pump–thaw cycles. Then CuCl (0.3 mmol) and CuCl₂ (if necessary) were added to the mixture. The system was again degassed by three freeze–pump–thaw cycles and sealed with a septum. The initiator (EBiB or EBP) was then added. The flask was placed in an oil bath maintained at the desired temperature [23]. The sample was diluted in acetone and filtered through a small plug of Al₂O₃. Then the solvent was evaporated at room temperature. Secondly, a mixture of macroinitiator (2 g, ≈0.1 mmol), FMA (2.1 g, ≈4 mmol), ligand (PMDETA) and solvent (cyclohexanone) was added to a 50 mL Schlenk flask equipped with a rubber septum and a stirring bar. After repeating the above steps, the product, P(MMA-BA-HEMA)-FMA, was prepared.

2.2. Preparation of superhydrophobic surfaces

P(MMA-BA-HEMA)-b-PFMA (0.04 g) was dissolved slowly in 0.015 mL acetone under ultrasonic environment. Then the mixture

was admixed in succession with 0.04 g L75 and 0.7 mL FHT, and was sonicated to accelerate the dissolution. The solution was directly cast-coated on a clean tin surface and then dried in an ambient environment.

2.3. Characterization

Shape and size of micelle particles were measured by transmission electron microscopy (TEM) (JEM-100CXII). The morphologies of the films were examined by scanning electron microscope (SEM) supplied by LEO (LEO 1530VP). An atomic force microscopy (AFM) (Dimension CSPM2000) was used to investigate the topography of thin film on glass. Images were acquired under ambient conditions in tapping mode using a Nanoprobe cantilever. Contact angle for water (WCA) and slide angle (SA) were measured with an OCA15 contact angle goniometer (Dataphysics Co., Germany). Each WCA and SA value was averaged from five measurements made at different positions of the film surface.

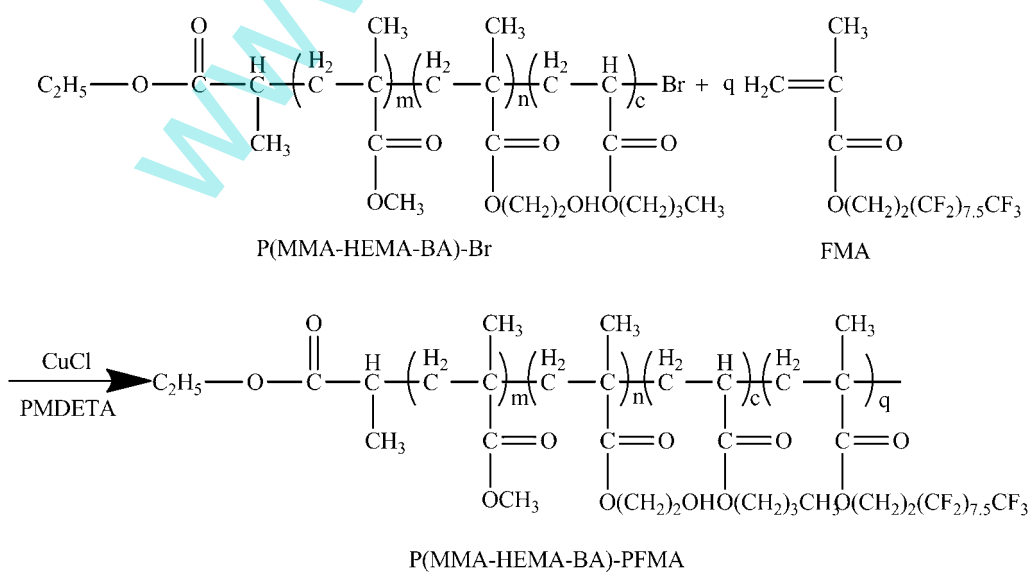
2.4. Test method of basic performances of superhydrophobic film

Analysis of adhesion grade was conducted according to adhesive attraction test methods in GB/T9286-1998 [14,15]. According to this standard, the blade is used to cut the film to make a lattice pattern on the film, with the number of both horizontal and vertical cuts being 6 in every cutting graph. The result is grade 0 when the cut line is smooth and no lattice drops off. The test was executed at least three times on one sample.

Hardness of the film was also examined with the pencils of different hardness going substantially parallel to the major axes of the test specimen. We carried out the experiment according to the Chinese national standard of GBT 6739-2006.

3. Results and discussion

The synthetic route of the copolymers is shown in Scheme 1. Chemical structures of the final products were verified by FTIR (Fig. 1) and ^1H NMR (Fig. 2). Fig. 1(a) shows the characteristic absorption peak located at 1446 cm^{-1} represents the CH_3 group in MMA [24]. The peaks at 2932 cm^{-1} and 2854 cm^{-1} are due to stretching vibration of $-\text{CH}_3$ and $-\text{CH}_2$ in HEMA, BA and FMA. The appearance of a wide absorption at 3435 cm^{-1} is stretching



Scheme 1. The procedure for preparing fluorinated block copolymer.

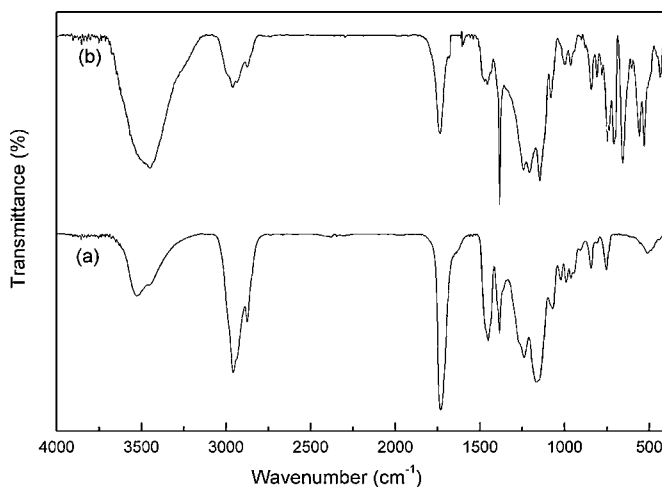


Fig. 1. FT-IR spectra of block copolymer (a) P(MMA-BMA-HEMA)-Br and (b) P(MMA-BMA-HEMA)-b-PFMA.

vibration of OH, indicating the existence of HEMA. The peaks at 496 cm⁻¹, 1237 cm⁻¹, 1724 cm⁻¹, 2977 cm⁻¹ are due to the characteristic absorption of C-Br, -O-C-O-, -C=O, and -CH₃. This suggests that the sample is the macro-initiator synthesized by MMA, HEMA and BA. The disappearance of the peak at 1640 cm⁻¹ indicates that no free monomer exists in the sample. Comparing Fig. 1(b) with Fig. 1(a), the first interest region lies between 1500 cm⁻¹ and 1000 cm⁻¹ of the FT-IR spectrum (b), which is dominated by bands associated with motions of the CF₂ group at 1260 cm⁻¹ ($\nu_a(CF_2) + r(CF_2)$) and 1160 cm⁻¹ ($\nu_b(CF_2) + d(CF_2)$) [25]. In addition, the band at 1220 cm⁻¹ is attributed to stretching and bending of the carbon skeleton of the fluorocarbon helix. The second interest region is that between 600 and 800 cm⁻¹. The first peak at 750 cm⁻¹ is due to the CF₃ group. The others are two medium bands at 666 and 711 cm⁻¹, resulting from a combination of rocking and wagging vibrations of the CF₂ group. It indicates that the synthetic product is the block polymer of P(MMA-BA-HEMA)-PFMA.

Fig. 2(a) and (b) are the ¹H NMR spectra of macromolecular initiator and fluorinated block copolymer. It can be seen from Fig. 2(b) that the peak at 3.61 ppm is attached to the -OCH₃ from MMA. The protons of the -OCH₂- are in the low field 3.94 and 3.85 ppm (peak

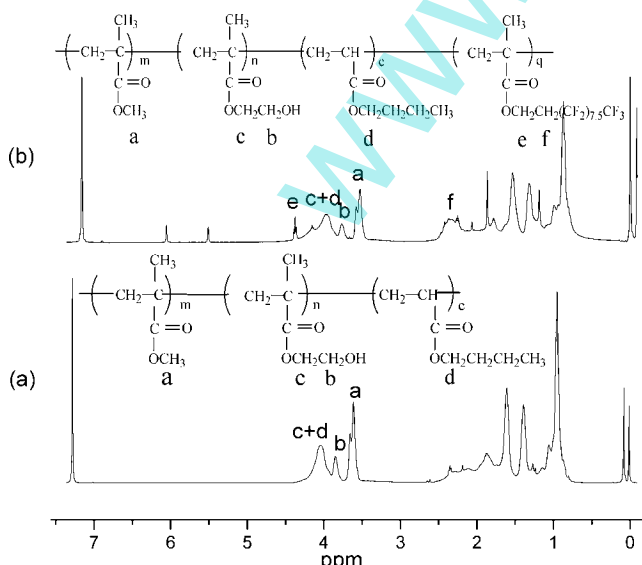


Fig. 2. ¹H NMR spectra of block copolymer (a) P(MMA-BMA-HEMA)-b-PFMA, (b) P(MMA-BMA-HEMA)-Br.

Table 1
Formulas of samples obtained with mixed solvent.

Sample	Fluorinated block copolymer (g)	L75 (g)	Acetone (μL)	FHT (μL)	Drying temperature (°C)
A	0.04	0.02	0	700	20
B	0.04	0.02	10	690	20
C	0.04	0.02	20	680	20
D	0.04	0.02	30	670	20
E	0.04	0.02	40	660	20
F	0.04	0.02	700	0	20
G	0.04	0	30	670	20
H	0.04	0.03	30	670	20

b, c and d) in BA and HEMA [26]. The protons at 4.43 ppm (peak e) and 2.35 ppm (peak f) are assigned to the -OCH₂- and -CH₂- in FMA. Compared to Fig. 2(a), the existence of the new peak e and f confirmed the successful synthesis of fluorinated block copolymer.

We also investigated the influence of solvents on film property, since solvents are demonstrated to seriously affect film formation process, wettability and mechanical performances of films [27]. Formula and performances of films obtained under different solvents are shown in Table 1 and Table 2. SEM images of the films and TEM images of the micelles are shown in Fig. 3 and Fig. 4.

When FHT was selected as solvent (sample A, Table 2), the WCA, hardness and adhesion grade of the film were $109.5 \pm 3.1^\circ$, 1H and 3 grade, respectively. This is because the FHT is a poor solvent for P(MMA-BA-HEMA) blocks, PFMA blocks and L75, there is no phase separation among polymers and no formation of micelles with core-shell structure when FHT is used as solvent and were only single-structure nanoparticles with an average diameter of 10–50 nm in solution (Fig. 3a). So the films obtained were smooth (Fig. 4a). Furthermore, the hydroxyl groups can hardly react with NCO groups in L75 because of the inhomogeneous mixing of block copolymer and L75, leading to a poor mechanical property.

The WCAs of Sample B, Sample C, Sample D and Sample E were $118.4 \pm 2.3^\circ$, $128.2 \pm 1.8^\circ$, $153.2 \pm 2.1^\circ$, and $128.5 \pm 2.9^\circ$, respectively. A small amount of microscale particles were formed when the content of acetone was relatively low (Fig. 4b and c). This is because FHT is a poor solvent for PFMA, acetone is a good solvent for P(MMA-BA-HEMA) and L75 and an insoluble solvent for PFMA. In mixed solvent with FHT as main solvent, a small quantity of acetone is beneficial for phase separation of block P(MMA-BA-HEMA) and PFMA to form micelle with core-shell structure. The chains of the PFMA will shrink and condense around P(MMA-BA-HEMA) cores, which contribute to film surface migration of PFMA rather than interpenetrating into neighboring multimolecular during the process of film formation. This results in the increase of roughness and decrease of surface energy of the film surface. Furthermore, the higher content of acetone is, the easier core-shell structure of micelle could be formed, and the higher WCA is.

The film of sample D exhibited medium mechanical properties (3H hardness, 2 grade adhesion) and high WCA of $153.2 \pm 2.1^\circ$, and the SA of this rough surface is ultra-low about 4° . This is because micelle particles with obvious core-shell structure were formed in

Table 2
Basic performances of copolymer films.

Items	WCA (°)	Hardness	Adhesion grade
Sample A	109.5 ± 3.1	1H	3 grade
Sample B	118.4 ± 2.3	1H	2 grade
Sample C	128.2 ± 1.8	2H	2 grade
Sample D	153.2 ± 2.1	3H	2 grade
Sample E	128.5 ± 2.9	3H	1 grade
Sample F	115.1 ± 3.5	5H	0 grade
Sample G	128.6 ± 1.8	H	2 grade
Sample H	132.7 ± 3.7	3H	2 grade

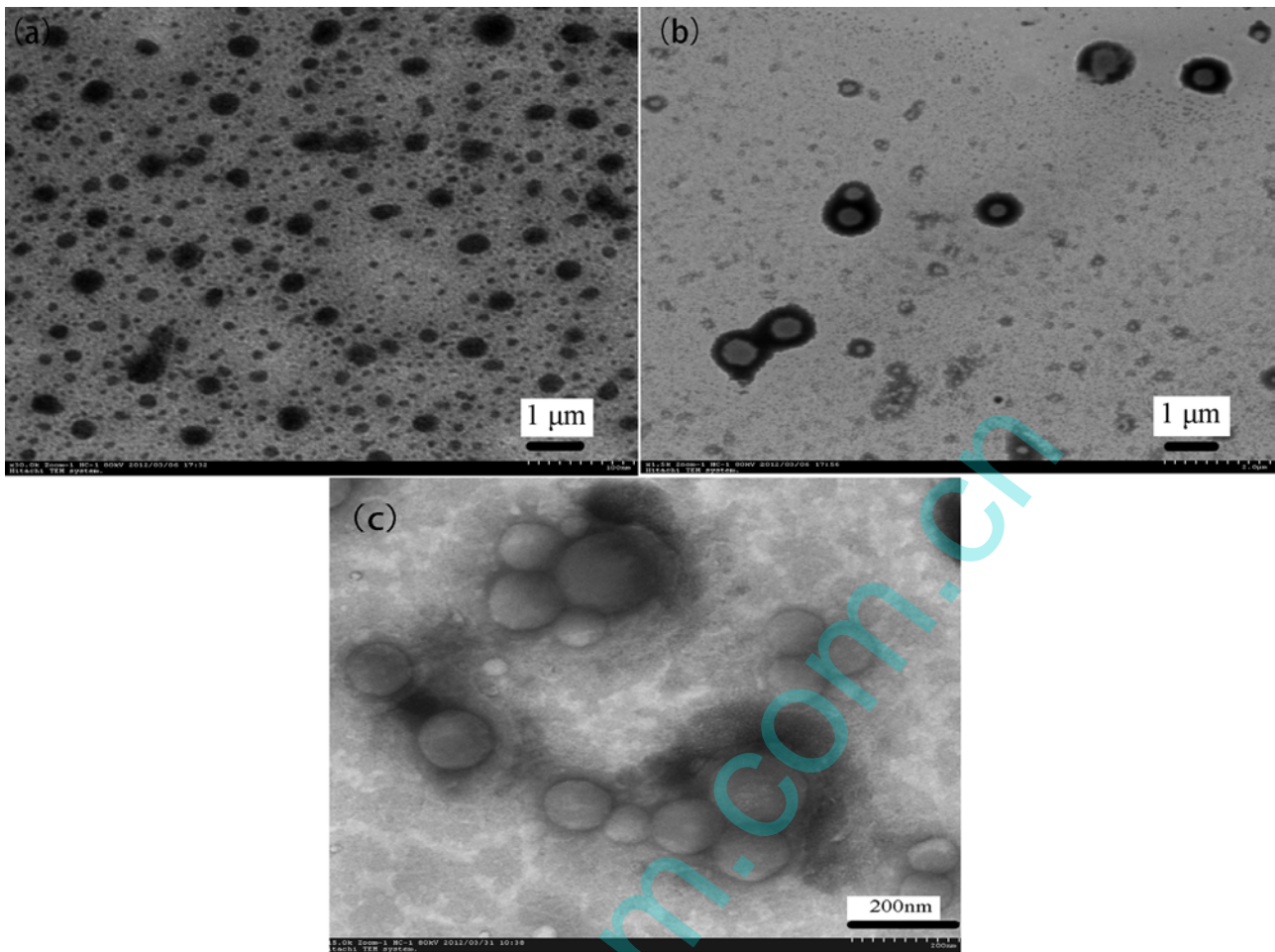


Fig. 3. TEM images of copolymer solution with different acetone content: (a) Sample A; (b) Sample D; (c) Sample F.

mixed solvent and the diameters were about 50–300 nm (Fig. 3b). The nanoscale micelle particles can aggregate to construct surface with micro/nano-scale hierarchical structure (Fig. 4d). This indicates that an appreciate amount of acetone contributes to the formation of the micelle particles with core-shell structure and improves the mechanical properties of the film.

The WCA of the film decreased to $128.5 \pm 2.9^\circ$ and the film exhibited better mechanical properties (hardness 3H and adhesion 1 grade) as acetone volume content further increased to 40/660 (sample E). This can be explained from the SEM image of Sample E (Fig. 4e), which reveals no nanoscale structure on the micro-papilla surface. It also can be seen from Table 2 that the mechanical properties of film increased with the acetone content. The reason is that increase of acetone content is beneficial for deformation and aggregation of micelles particles, and assists the reaction between OH group and NCO group.

When only acetone was used as solvent (sample F), the hardness and adhesion grade of the film were up to 5H and 0 grade, where WCA was just $115.1 \pm 3.5^\circ$. This is because the acetone is a good solvent for P (MMA-BA-HEMA) blocks and a non-solvent for PFMA blocks, the micelles with P (MMA-BA-HEMA) blocks as shell and PFMA blocks as core are easily formed in acetone, which can be seen from Fig. 3c. However, the shell formed by P (MMA-BA-HEMA) block is very thin due to chains of the P (MMA-BA-HEMA) blocks stretching in acetone. It is helpful for aggregation and interpenetration between the micelle particles, leading to smooth surface. Furthermore, the hydroxyl groups of P (MMA-BA-HEMA) block copolymer are on the shell of the micelle and can easily react with

NCO group of L75. The crosslinking products restrict PFMA blocks migration from the interior of the micelles to the surface. So the film exhibited low WCA and good mechanical performances [17].

For sample G and H, which contains no and 0.03 g L75, the WCA of film were only $128.6 \pm 1.8^\circ$ and $132.7 \pm 3.7^\circ$, the hardness were H and 3H, adhesion was all 2 grade. This is because the polarity of L75 is similar to P (MMA-BA-HEMA) block, absence and excessive content of L75 is bad for formation of core-shell structure of micelle and that no crosslinking reaction between –OH and –NCO or excessive content of L75, leading to low WCA and bad hardness. It suggests that the ratio of acetone to FHT in the mixed solvent and the binder L75 affect the film hydrophobicity and mechanical property seriously.

The drying temperature dramatically affects evaporation rate of solvent and migration rate of polymer chains, so as to the hydrophobicity and mechanical property. The WCA and mechanical property of the films (sample D) at different drying temperature are shown in Fig. 5. Fig. 5 shows that the WCA increased initially, and then decreased with drying temperature. The WCA was up to maximum of $153.2 \pm 2.1^\circ$ when drying at 20°C . This is because solvent evaporation rate and phase separation rate were appropriate for aggregation of micelles and formed a micro/nano scale binary hierarchical structure at 20°C . However, when the film was dried at 10°C , the WCA was just 136°C . The first reason is that from Clausius-Clapeyron relation

$$\ln \frac{P_1}{P_2} = -\frac{L}{R} \left(\frac{1}{T_1} - \frac{1}{T_2} \right) \quad (1)$$

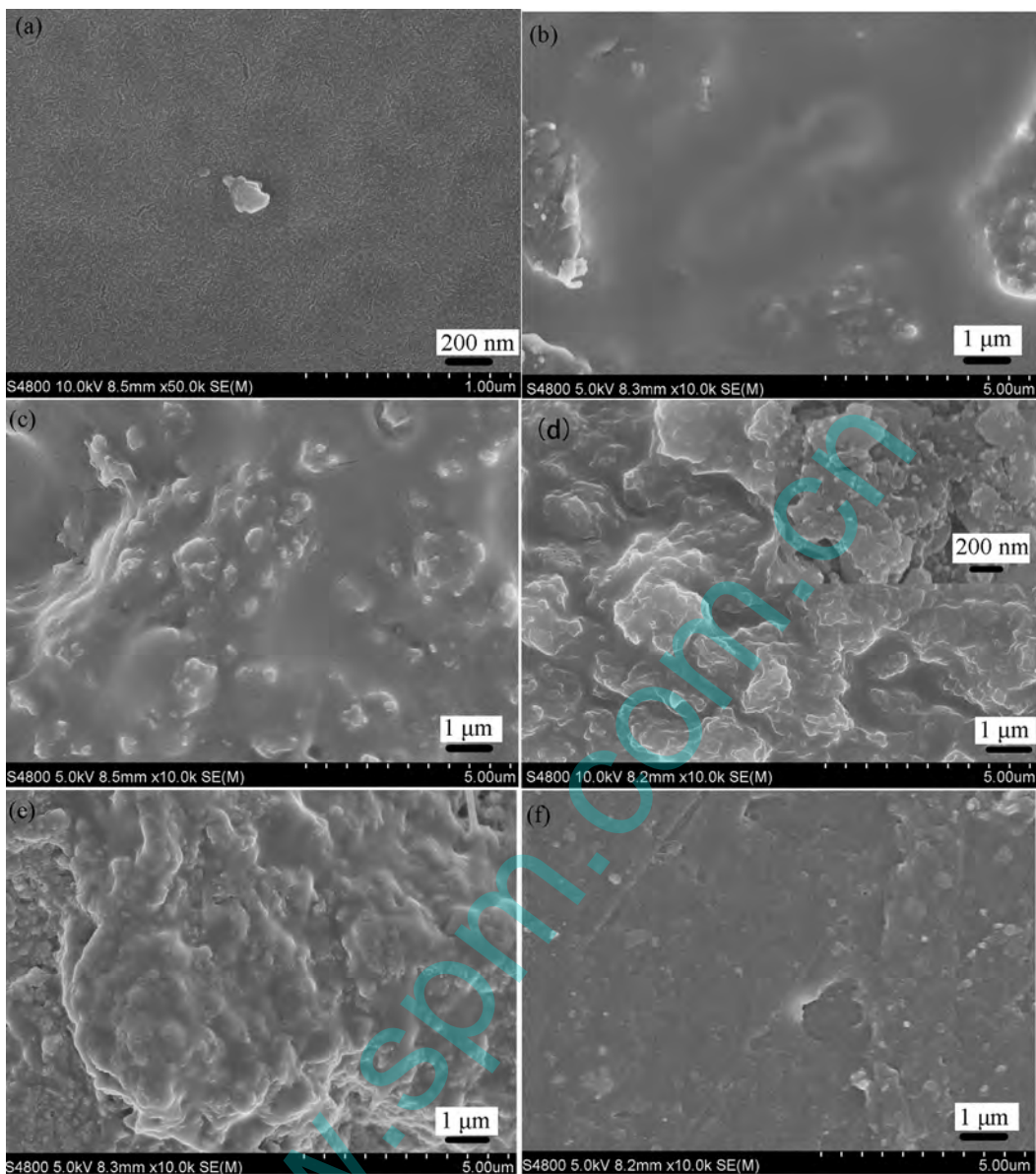


Fig. 4. SEM images of copolymer films obtained with different mixed solution in copolymer solution: (a) Sample A; (b) Sample B; (c) Sample C; (d) Sample D; (e) Sample E; (f) Sample F.

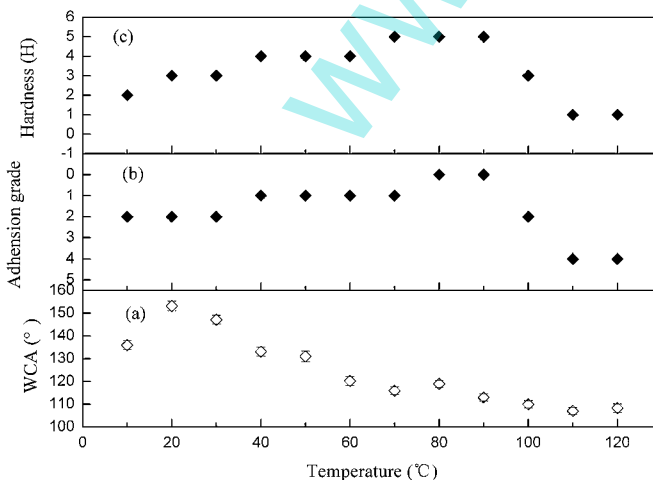


Fig. 5. The relationship between WCA, adhesion grade, hardness of the film and temperature.

where P is the pressure, R is the specific gas constant, L is the specific latent heat of the substance and T is Kelvin temperature, we can know that ratio of acetone saturation vapor pressure at 20 °C to 10 °C is 2.13 (based on 57 °C boiling point of acetone), which is lower than that of FHT at 2.41 (based on 133 °C boiling point of FHT). It means lower temperature has less effects on the relative volatilization of acetone and it is beneficial for the evaporation of acetone prior to FHT at 10 °C. The micelles lose core-shell structure before deformation and aggregation due to the absence of acetone. The other one is because low temperature is bad for the surface migration of fluorine groups. When the drying temperature was raised beyond 30 °C, hydrophobicity of the films also dramatically decreased. This phenomenon happens because the deformation and migration of the copolymer chains is more serious at 30 °C, resulting in smooth surfaces.

As been shown in curve b and curve c of Fig. 5, the adhesion grade and hardness increased with drying temperature and reached the maximum at 0 grade and 5H when the drying temperature was 80 °C. This is because the reaction activity of L75 increases

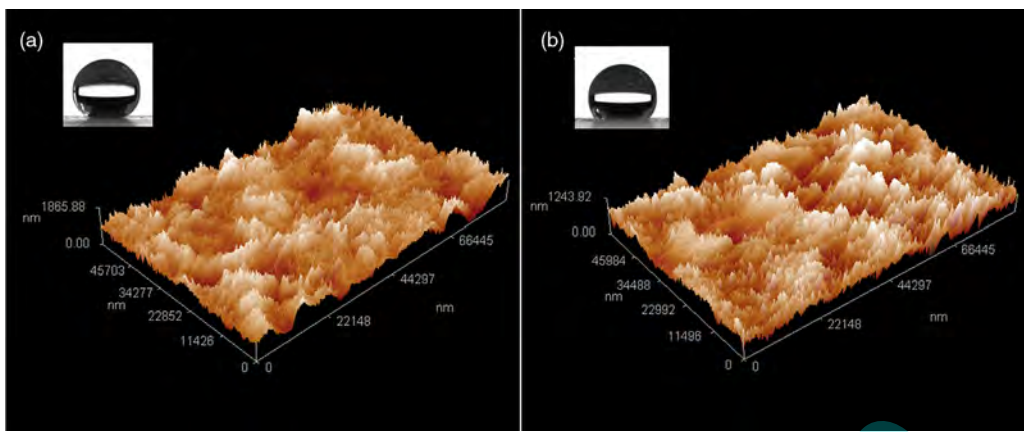


Fig. 6. AFM images of copolymer films obtained with different acetone content in copolymer solution: (a) Sample D; (b) Sample E.

with the temperature and reaches the highest at 80 °C, and the reaction degree between hydroxyl groups and isocyanate groups is the highest at 80 °C. The mechanical properties decreased when the drying temperature further increased, caused by the low reaction degree between hydroxyl groups and isocyanate. According to GB/T-9286-1998, the adhesion can meet the requirement in practical application when it is not lower than 2 grade [13]. Table 2 and Fig. 5 show that the superhydrophobic films with mechanical properties satisfying practical application can be obtained when the volume content of acetone is 30/670 in mixed solvent, with a drying temperature of 20 °C.

Surface roughness can be assessed by surface roughness factor (r), which is the ratio of actual area of rough surface to the geometric projected area. Two distinct models have been proposed to explain this: the Wenzel model and the Cassie model. The Wenzel model describes a roughness regime in which both advancing WCA and WCA hysteresis (WCAH) increase as r increases (water penetrates into the surface cavity). The Cassie model describes that, as r further increases passing a critical level, the water receding angle also increases dramatically (water does not penetrate into the surface cavity; there is an air pocket between the water droplet and the solid surface), thus minimizing the WCA. The surface morphology of the sample D and sample E were observed using AFM as shown in Fig. 6. The results of surface roughness factor (r , $r = 1 + S_{dr}$, S_{dr} is surface area ratio, which is the ratio between the interfacial and projected areas) was obtained from AFM software analyses. The roughness factor of sample D and sample E are 1.33 and 1.21. The Wenzel's model is showed as follows:

$$\cos \theta^w = r \cos \theta \quad (2)$$

where θ^w and θ are the apparent WCA and the WCA of a flat fluorinated surface, respectively. The apparent water contact angle calculated from the Wenzel's model (124.3° and 120.9°, based on the 115.1° WCA of a flat fluorinated surface) is much lower than experimental value obtained (153.2 ± 2.1° and 128.2 ± 1.8°) in this work. This indicates that a composite surface may be formed to allow air pockets to exist between the water droplet and the solid surface. For a composite surface, water contact angle is described by the Cassie–Baxter equation as follows:

$$\cos \theta_r^c = f \cos \theta + f - 1 \quad (2)$$

where f is the area fraction of the solid in contact with the liquid. The value of f was calculated to be 0.187. This result implies that water did not penetrate the surface grooves on the films.

4. Conclusion

In summary, we have successfully prepared superhydrophobic surface by casting micelle particles of fluorinated crosslinkable block copolymer and curing agent L75 in the mixture of acetone and FHT. Our study shows that film hydrophobicity is affected by ratio of acetone to FHT, as well as the content of L75 and drying temperature. The introduction of a small quantity of acetone contributes to the formation of micelle particles, where a core-shell structure leads to a rough film. However, the excessive acetone makes the size of micelle particles larger, resulting in a smooth surface of the film. It is also found that mechanical properties of the film can be improved by the addition of crosslinking curing agent L75. The film with the highest superhydrophobicity in this study has a WCA at 153.2 ± 2.1° and sliding angle of 4° and improved mechanical performance that satisfied practical application (e.g. self-cleaning). The method developed in this paper is simple, low-cost and can be extended to fabricate surface in large-area for practical applications.

Acknowledgements

We are grateful for the financial support from National Natural Science Foundation of China (Grant No. 21176091 and No. 21376093), team project of Natural Science Foundation of Guangdong Province (Grant No. S2011030001366) and Fundamental Research Funds for the Central Universities (Grant No. 2013ZZ074).

References

- [1] X. Deng, L. Mammen, H.J. Butt, D. Vollmer, *Science* 335 (2012) 67–70.
- [2] S. Nishimoto, B. Bhushan, *RSC Adv.* 3 (2013) 671–690.
- [3] A. Lafuma, D. Quéré, *Nat. Mater.* 2 (2003) 457–460.
- [4] C.W. Peng, K.C. Chang, C.J. Weng, C.H. Lai, C.H. Hsu, S.C. Hsu, Y.Y. Hsu, W.I. Hung, Y. Wei, J.M. Yeh, *Electrochim. Acta* 95 (2013) 192–199.
- [5] L. Feng, S.H. Li, Y.S. Li, H.J. Li, L.J. Zhang, Y.L. Song, B.Q. Liu, J. Liang, D.B. Zhu, *Adv. Mater.* 14 (2014) 1857–1860.
- [6] J. Fresnais, J.P. Chapel, F. Poncin-Epaillard, *Surf. Coat. Technol.* 22 (2006) 5296–5305.
- [7] T. Kiyoharu, K. Kaori, M. Atsunori, M. Tsutomu, *J. Sol-Gel Sci. Technol.* 26 (2003) 705.
- [8] S.S. Latthe, H. Imai, V. Ganesan, C. Kappenstein, A.V. Rao, *J. Sol-Gel Sci. Technol.* 53 (2010) 208–215.
- [9] A. Nakajima, A. Fujishima, K. Hashimoto, T. Watanabe, *Adv. Mater.* 11 (1999) 1365–1368.
- [10] M. Im, H. Im, J.H. Lee, J.B. Yoon, Y.K. Choi, *Soft Matter* 6 (2010) 1401–1404.
- [11] C.W. Tu, C.H. Tsai, C.F. Wang, S.W. Kuo, F.C. Chang, *Macromol. Rapid Commun.* 28 (2007) 2262–2266.
- [12] P. Roach, N.J. Shirtcliffe, M. Newton, *Soft Matter* 4 (2008) 224–240.
- [13] L. Cao, D. Gao, *Faraday Discuss.* 146 (2010) 57–65.
- [14] X.F. Wen, Y. Liu, Z.J. Xu, J.X. Yang, P.H. Pi, Z.Q. Cai, J. Cheng, Z.R. Yang, *Soft Mater.* 10 (2012) 415.

- [15] J.X. Yang, P.H. Pi, X.F. Wen, D.F. Zheng, M.Y. Xu, J. Cheng, Z.R. Yang, *Appl. Surf. Sci.* 255 (2009) 3507.
- [16] H. Yabu, M. Shimomura, *Chem. Mater.* 17 (2005) 5231–5234.
- [17] T.P. Lodge, *Macromol. Chem. Phys.* 204 (2003) 265.
- [18] Q.D. Xie, G.Q. Fan, N. Zhao, X.L. Guo, J. Xu, J.Y. Dong, L.Y. Zhang, Y.J. Zhang, C.C. Han, *Adv. Mater.* 16 (2004) 1830.
- [19] Q.D. Xie, J. Xu, L. Feng, L. Jiang, W.H. Tang, X.D. Luo, C.C. Han, *Adv. Mater.* 16 (2004) 302.
- [20] V.D. Deepak, S.K. Asha, *J. Phys. Chem.* 110 (2006) 21450.
- [21] X.F. Wen, Q.H. Xie, Y.L. Lu, Z.Q. Cai, P.H. Pi, J. Cheng, Z.R. Yang, *J. Chem. Eng. Chin. Univ.* 26 (1012) 505 (in Chinese).
- [22] Y.Q. Wang, Y. Shi, L.J. Pan, M. Yang, L.L. Peng, S. Zong, Y. Shi, G.H. Yu, *Nanoletters* 14 (2014) 4803–4809.
- [23] X.F. Wen, J.L. Lan, Y. Liu, P.H. Pi, Z.Q. Cai, S.P. Xu, L.J. Zhang, Y. Qian, *Polym. Int.* 63 (2014) 1238.
- [24] B. Wu, X.X. Li, J. Jiao, P.P. Wu, Z.W. Han, *J. East China Univ. Sci. Technol.* 27 (60) (2001) (in Chinese).
- [25] J. Schneider, C. Erdelen, H. Ringsdorf, J.F. Rabolt, *Macromolecules* 22 (1989) 3475.
- [26] S.L. Lin, X.F. Wen, Z.Q. Cai, P.H. Pi, D.F. Zheng, J. Cheng, L.J. Zhang, Y. Qian, Z.R. Yang, *Phys. Chem. Chem. Phys.* 13 (2011) 17323.
- [27] H.Y. Erbil, A.L. Demirel, Y. Avci, O. Mert, *Science* 299 (2003) 1377.